Internat. J. Math. & Math. Sci.
Vol. 7 No. 4 (1984) 765-784

ASYMPTOTIC SOLUTION OF THE LOW REYNOLDS-NUMBER FLOW BETWEEN TWO CO-AXIAL CONES OF COMMON APEX

M.A. SERAG-ELDIN AND Y.K. GAYED

Mechanical Engineering Department
Faculty of Engineering, Cairo University
Cairo, EGYPT

(Received March 29, 1979)

ABSTRACT. The paper is concerned with the axi-symmetric, incompressible, steady, laminar and Newtonian flow between two, stationary, conical-boundaries, which exhibit a common apex but may include arbitrary angles. The flow pattern and pressure field are obtained by solving the pertinent Navier-Stokes' equations in the spherical coordinate system. The solution is presented in the form of an asymptotic series, which converges towards the creeping flow solution as a cross-sectional Reynolds-number tends to zero. The first term in the series, namely the creeping flow solution, is given in closed form; whereas, higher order terms contain functions which generally could only be expressed in infinite series form, or else evaluated numerically. Some of the results obtained for converging and diverging flows are displayed and they are demonstrated to be plausible and informative.

KEY WORDS AND PHRASES. Asymptotic solution, low Reynolds-number, conical boundaries, axi-symmetric flow, incompressible flow, laminar flow, Navier-Stokes equation.

1980 MATHEMATICS SUBJECT CLASSIFICATION CODES. 16005.

1. INTRODUCTION.

1.1 Problem Statement

The problem considered is that of predicting the steady, incompressible, laminar and Newtonian flow inside the passage formed between two, co-axial, fixed cones of common apex, Figure 1. The apex is the source of the diverging flow and the sink of the converging one. The flow region of interest exhibits low absolute values of a cross-sectional R_N defined by $\frac{q}{r\nu}$. The flow is assumed axi-symmetric, and both swirl and body forces are absent.

The velocity and pressure profiles are sought at different cross-sections, for

various apex angles of each cone.

1.2 Solution Technique

The method of solution employed here is an indirect one, in which the dependent variables are expanded in a finite series whose coefficients are unknown functions to be determined by substitution in the equations of motion. The first term in the series is the creeping flow solution; as the cross-sectional R_N decreases, the solution tends asymptotically towards the first term.

Some of the mathematical properties of asymptotic series solutions may be found in, for example, Morse and Feshbach [1].

1.3 Previous Work

Historically, various authors have employed asymptotic series to solve duct flow problems. Among these, Peube [2] was the first to obtain an asymptotic solution for the velocity and pressure distribution inside two parallel disks. Later, Ackerberg [3] derived an asymptotic solution for the flow inside a cone, whereas Rice and McAlister [4] obtained the solution for the special case of the throughflow between co-axial co-rotating cones having the same semi-vertex angle in terms of the already existing solution for the flow between parallel disks.

2. MATHEMATICAL MODEL.

2.1 The Governing Equations

The mathematical model comprises the Navier-Stokes momentum equations and the equation of continuity. The spherical system of co-ordinates (r,θ,ϕ) is adopted, in order to simplify the expression of the boundary conditions. Due to axial symmetry and absence of swirl, all terms in both ϕ and v_ϕ are omitted. Thus the governing equations are:

the r-momentum equation

$$v_r \frac{\partial v_r}{\partial r} + \frac{v_\theta}{r}\frac{\partial v_r}{\partial \theta} - \frac{v_\theta^2}{r} = -\frac{1}{\rho}\frac{\partial p}{\partial r} + \nu\left(\nabla^2 v_r - \frac{2v_r}{r^2} - \frac{2}{r^2}\frac{\partial v_\theta}{\partial \theta} - 2v_\theta \frac{\cot\theta}{r^2}\right), \tag{2.1}$$

the θ-momentum equation

$$v_r \frac{\partial v_\theta}{\partial r} + \frac{v_\theta}{r}\frac{\partial v_\theta}{\partial \theta} + \frac{v_r v_\theta}{r} = -\frac{1}{\rho r}\frac{\partial p}{\partial \theta} + \nu\left(\nabla^2 v_\theta + \frac{2}{r^2}\frac{\partial v_r}{\partial \theta} - \frac{v_\theta}{r^2 \sin^2\theta}\right), \tag{2.2}$$

and the equation of continuity

$$\frac{\partial v_r}{\partial r} + \frac{2v_r}{r} + \frac{1}{r}\frac{\partial v_\theta}{\partial \theta} + v_\theta \frac{\cot\theta}{r} = 0, \tag{2.3}$$

where

$$\nabla^2 = \frac{1}{r^2}\frac{\partial}{\partial r}\left(r^2 \frac{\partial}{\partial r}\right) + \frac{1}{r^2 \sin\theta}\frac{\partial}{\partial \theta}\left(\sin\theta \frac{\partial}{\partial \theta}\right). \tag{2.4}$$

2.2 The Boundary Conditions

The non-slip conditions at the walls state that:

$$\begin{aligned} v_r &= 0 \quad \text{at} \quad \theta = \theta_1 \quad \text{and} \quad \theta = \theta_2 \\ v_\theta &= 0 \quad \text{at} \quad \theta = \theta_1 \quad \text{and} \quad \theta = \theta_2 \ . \end{aligned} \tag{2.5}$$

In addition to these conditions, continuity of the flow dictates that q is the same at all cross-sections. q is given by

$$q = r^2 \int_{\theta_1}^{\theta_2} v_r \ \sin\theta \ .d\theta \tag{2.6}$$

where q is positive for diverging flows and negative for converging ones.

2.3 The ψ-Equation and Boundary Conditions

Introducing a stream function $\psi(r,Z)$ defined by

$$v_r = -\frac{1}{r^2}\frac{\partial\psi}{\partial Z} \ , \quad v_\theta = \frac{-1}{r\sqrt{1-Z^2}}\frac{\partial\psi}{\partial r} \tag{2.7}$$

where $Z = \cos\theta$, the continuity equation is identically satisfied and the momentum equations are reduced to

$$\frac{1}{\rho}\frac{\partial p}{\partial r} = \frac{1}{r^4}\frac{\partial(\psi,\partial\psi/\partial Z)}{\partial(r,Z)} + \frac{1}{r^3}\left[\frac{2}{r^2}\left(\frac{\partial\psi}{\partial Z}\right)^2 + \frac{1}{1-Z^2}\left(\frac{\partial\psi}{\partial r}\right)^2\right] - \frac{\nu}{r^2}\frac{\partial(D^2\psi)}{\partial Z} \tag{2.8a}$$

$$\frac{1}{\rho}\frac{\partial p}{\partial Z} = -\frac{1}{r^2(1-Z^2)}\frac{\partial(\psi,\partial\psi/\partial r)}{\partial(r,Z)} - \frac{Z}{r^2(1-Z^2)^2}\left(\frac{\partial\psi}{\partial r}\right)^2 + \frac{\nu}{1-Z^2}\frac{\partial(D^2\psi)}{\partial r} \ . \tag{2.8b}$$

Furthermore, by eliminating the pressure terms from Equations (2.8a) and (2.8b), the following equation results for ψ:

$$\frac{1}{r^2}\frac{\partial(\psi,D^2\psi)}{\partial(r,Z)} + 2\frac{D^2\psi}{r^2}\left(\frac{Z}{1-Z^2}\frac{\partial\psi}{\partial r} + \frac{1}{r}\frac{\partial\psi}{\partial Z}\right) = \nu D^4\psi \tag{2.9a}$$

where

$$D^4 = D^2 \ D^2, \quad \text{and} \quad D^2 = \frac{\partial^2}{\partial r^2} + \frac{1-Z^2}{r^2}\frac{\partial^2}{\partial Z^2} \ . \tag{2.9bc}$$

In terms of the new dependent variable ψ the boundary conditions reduce to:

$$\psi(r,Z_1) = \psi_1 \tag{2.10a}$$

$$\psi(r,Z_2) = \psi_2 \tag{2.10b}$$

$$\frac{\partial\psi}{\partial\theta} = 0 \quad \text{at} \quad \theta = \theta_1 \quad \text{and} \quad \theta = \theta_2 \tag{2.10cd}$$

$$q = \psi_2 - \psi_1 \ . \tag{2.10e}$$

2.4 The Dimensionless Forms

Introducing the dimensionless variables R, V_R, V_θ, Ψ and P defined by

$$R = \frac{r\nu}{q} , \quad V_R = \frac{qv_r}{\nu^2} , \quad V_\theta = \frac{qv_\theta}{\nu^2} , \quad \Psi = \frac{\psi}{q} , \quad P = \frac{pq^2}{\rho\nu^4} \tag{2.11}$$

in Equations (2.7)-(2.10), the following equations result for the dimensionless variables:

$$V_R = -\frac{1}{R^2}\frac{\partial\Psi}{\partial Z} \tag{2.12a}$$

$$V_\theta = -\frac{1}{R\sqrt{1-Z^2}}\frac{\partial\Psi}{\partial R} \tag{2.12b}$$

$$\frac{1}{R^2}\frac{\partial(\Psi,D^2\Psi)}{\partial(R,Z)} + \frac{2\,D^2\Psi}{R^2}\left(\frac{1}{1-Z^2}\frac{\partial\Psi}{\partial R} + \frac{1}{R}\frac{\partial\Psi}{\partial Z}\right) = D^4\Psi \tag{2.13}$$

where D^2 is the operator of (2.9c) with R replacing r.

$$\frac{\partial P}{\partial R} = \frac{1}{R^4}\frac{\partial(\Psi,\partial\Psi/\partial Z)}{\partial(R,Z)} + \frac{1}{R^3}\left|\frac{2}{R^2}\left(\frac{\partial\Psi}{\partial Z}\right)^2 + \frac{1}{1-Z^2}\left(\frac{\partial\Psi}{\partial R}\right)^2\right| - \frac{1}{R^2}\frac{\partial(D^2\Psi)}{\partial Z} \tag{2.14a}$$

$$\frac{\partial P}{\partial Z} = -\frac{1}{R^2(1-Z^2)}\frac{\partial(\Psi,\partial\Psi/\partial R)}{\partial(R,Z)} - \frac{Z}{R^2(1-Z^2)^2}\left(\frac{\partial\Psi}{\partial R}\right)^2 + \frac{1}{1-Z^2}\frac{\partial(D^2\Psi)}{\partial R} \tag{2.14b}$$

Setting $\psi_1 = 0$, then $\psi_2 = q$ and dimensionless boundary conditions become

$$\Psi(R,Z_1) = 0, \quad \Psi(R,Z_2) = 1 \tag{2.15ab}$$

$$\left(\frac{\partial\Psi}{\partial Z}\right) = 0 \qquad \text{at} \qquad Z = Z_1 \quad \text{and} \quad Z = Z_2 \ . \tag{2.15cd}$$

Equations (2.11)-(2.15) constitute the mathematical model of the problem. The solution of Equation (2.13) for the boundary conditions specified by equations (2.15) yields the Ψ distribution from which, with the help of Equations (2.14, 2.12), the P, V_R and V_θ profiles are derived.

3. THE CREEPING FLOW SOLUTION

3.1 Differential Equation and Boundary Conditions.

At large values of R, the flow is creeping, i.e. the inertia terms are of a smaller magnitude than the viscous ones. If the inertia terms of Equation (2.13) are neglected altogether, then a purely radial-flow solution, $\Psi = f_o(Z)$, will satisfy the resulting equation. The flow will then be governed by the following total differential-equation for $f_o(Z)$:

$$\frac{d^2}{dZ^2}\left[(1-Z^2)\,f_o''\right] + 6\,f_o'' = 0 \tag{3.1}$$

coupled with the boundary conditions:

$$f_o(Z) = 0 \qquad \text{at} \qquad Z = Z_1 \tag{3.2a}$$

$$f_o(Z) = 1 \qquad \text{at} \qquad Z = Z_2 \tag{3.2b}$$

$$f_o'(Z) = 0 \qquad \text{at} \qquad Z = Z_1 \quad \text{and} \quad Z = Z_2 \ . \tag{3.2cd}$$

3.2 Solution of the Differential Equation.

The general solution of equation (3.1) is derived in Appendix A; it gives $f_o(Z)$, $f_o'(Z)$ in terms of Legendre-Functions (see for e.g. Abramowitz [5]) and their derivatives, as follows:

$$f_o(Z) = \frac{1}{6}\{(Z^2 - 1)[C_o P_2'(Z) + D_o Q_2'(Z)] + A_o Z + B_o\} \tag{3.3a}$$

$$f_o'(Z) = \frac{A_o}{6} + C_o P_2(Z) + D_o Q_2(Z) \tag{3.3b}$$

where A_o, B_o, C_o and D_o are arbitrary constants. In order to satisfy the boundary conditions expressed in Equation (3.2), these constants are determined from the following relations:

$$\frac{D_o}{C_o} = \frac{P_2(Z_1) - P_2(Z_2)}{Q_2(Z_2) - Q_2(Z_1)} \tag{3.4a}$$

$$\frac{A_o}{C_o} = -6\{\frac{D_o}{C_o} Q_2(Z_1) + P_2(Z_1)\} \tag{3.4b}$$

$$\frac{B_o}{C_o} = (1 - Z_1^2)[P_2'(Z_1) + \frac{D_o}{C_o} Q_2'(Z_1)] - \frac{A_o}{C_o} Z_1 \tag{3.4c}$$

$$C_o = \frac{6}{\{(Z_2^2 - 1)[P_2'(Z_2) + \frac{D_o}{C_o} Q_2'(Z_2)] + \frac{A_o}{C_o} Z_2 + \frac{B_o}{C_o}\}} \tag{3.4d}$$

4. THE ASYMPTOTIC SERIES SOLUTION.

4.1 The Ψ Series

For large values of R, it seems reasonable to postulate an asymptotic expansion for Ψ such that the series converges to the creeping flow solution as $R \to \infty$. Thus, the following asymptotic series is postulated for Ψ

$$\Psi(R,Z) \sim \sum_{n=o}^{k} \frac{f_n(Z)}{R^n} \tag{4.1}$$

where k is the number of terms of the series chosen according to the value of R and the required accuracy. Here, no rigourous proof is given of the asymptotic nature of the solutions. However, for the solutions obtained, the series converges for a finite number of terms k, the value of k increasing with R, thus depicting a typical asymptotic expansion behavior.

The first term in the series is the creeping flow solution $f_o(Z)$; whereas, the subsequent coefficients of R^{-n}, namely $f_n(Z)$, are unknown functions of Z to be determined in the following sections.

4.2 Differential Equation and Boundary Condition for $f_n(Z)$.

In order to evaluate $f_n(Z)$ for $1 \le n \le k$, the expressions for $\Psi(R,Z)$ (postulated in Equation (4.1)) and its derivatives are substituted in Equation (2.13) and the summation of the coefficients of like powers of R are equated to zero, thus yielding the following differential-equations for $f_n(Z)$:

$$(1 - Z^2)^2 f_n^{IV} - 4Z(1 - Z^2) f_n''' + 2(n + 1)(n + 2)(1 - Z^2) f_n'' + n(n + 1)(n + 2)(n + 3) f_n = F_n(Z) \qquad (4.2)$$

where

$$F_n(Z) \equiv \sum_{s=o}^{n-1} f'_{n-1-s} (s + 4)[s(s + 1) f_s + (1 - Z^2) f_s''] - \sum_{s=o}^{n-1} (n - 1 - s) f_{n-1-s} [s(s + 1) f'_s + (1 - Z^2) f_s''' + (s + 1) \frac{2Z}{1 - Z^2} f_s] \; . \qquad (4.3)$$

The boundary conditions for Equation (4.2) are obtained by substituting the expressions for $\Psi(R,\theta)$ and its derivatives in the expressions for the $\Psi(R,\theta)$ boundary-conditions, Equations (2.15). The resulting boundary conditions for all values of $n \ge 1$, are:

$$f'_n(Z) = 0 \quad \text{at} \quad Z = Z_1 \quad \text{and} \quad Z = Z_2 \qquad (4.4ab)$$

$$f_n(Z) = 0 \quad \text{at} \quad Z = Z_1 \quad \text{and} \quad Z = Z_2 \; . \qquad (4.4cd)$$

4.3 Evaluation of $f_n(Z)$

In general, it is not possible to evaluate $f_n(Z)$ in closed form. Two other possibilities present themselves: either numerical integration or an analytic solution comprising an infinite series.

Numerical integration of equation (4.2) is a simple task since it merely entails the successive solutions of linear, total differential-equations. The differential equations are first cast in their corresponding finite-difference form, and the resulting system of algebraic equations are then solved by any of the well known solution algorithms. The particular one adopted here, was an available computer-library subroutine.

The analytic solution is given by the sum of the complementary function (solution of the homogeneous equation) and any particular solution of the full equation, $Y_n(Z)$. Thus from Appendix C it is deduced that the analytic solution is expressed by:

$$f_n(Z) = - (1 - Z^2) \frac{A_n P'_n(Z) + B_n Q'_n(Z)}{n(n + 1)} + \frac{C_n P'_{n+2}(Z) + D_n Q'_{n+2}(Z)}{(n + 2)(n + 3)} + Y_n(Z) \qquad (4.5a)$$

and

$$f_n'(Z) = A_n P_n(Z) + B_n Q_n(Z) + C_n P_{n+2}(Z) + D_n Q_{n+2}(Z) + Y_n'(Z) \tag{4.5b}$$

where A_n, B_n, C_n and D_n are constants which are determined from the solution of the following matrix:

$$\begin{bmatrix} P_n(Z_1) & Q_n(Z_1) & P_{n+2}(Z_1) & Q_{n+2}(Z_1) \\ P_n(Z_2) & Q_n(Z_2) & P_{n+2}(Z_2) & Q_{n+2}(Z_2) \\ \dfrac{P_n'(Z_1)}{n(n+1)} & \dfrac{Q_n'(Z_1)}{n(n+1)} & \dfrac{P_{n+2}'(Z_1)}{(n+2)(n+3)} & \dfrac{Q_{n+2}'(Z_1)}{(n+2)(n+3)} \\ \dfrac{P'(Z_2)}{n(n+1)} & \dfrac{Q_n'(Z_2)}{n(n+1)} & \dfrac{P_{n+2}'(Z_2)}{(n+2)(n+3)} & \dfrac{Q_{n+2}'(Z_2)}{(n+2)(n+3)} \end{bmatrix} \begin{bmatrix} A_n \\ B_n \\ C_n \\ D_n \end{bmatrix} \begin{bmatrix} -Y_n'(Z_1) \\ -Y_n'(Z_2) \\ \dfrac{Y_n(Z_1)}{1 - Z_1^2} \\ \dfrac{Y_n(Z_2)}{1 - Z_2^2} \end{bmatrix} .$$

In general it is not possible to derive a closed form expression for $Y_n(Z)$. Thus Adams' method is employed to obtain a Taylors' series expansion for $Y_n(Z)$ about Z_2, i.e.,

$$Y_n(Z) = \sum_{m=o}^{\infty} b_{n,m}(Z - Z_2)^m \tag{4.6}$$

where $$b_{n,o} = Y_n(Z_2), \ \ldots, \ b_{n,m} = Y_n^{(m)}(Z_2)/m! \tag{4.7}$$

Four of the coefficients b_m may be chosen ad lib to produce any desired particular solution. A suitable choice is:

$$b_{n,o} = b_{n,1} = b_{n,2} = b_{n,3} = 0 \quad . \tag{4.8}$$

Subsequent coefficients are then derived by successive substitution and differentiation of Equation (4.2). The following values result for $b_{n,4}$, $b_{n,5}$, $b_{n,6}$ and $b_{n,7}$:

$$b_{n,4} = 0 \tag{4.9a}$$

$$b_{n,5} = \frac{F_n'(Z_2)}{120(1 - Z_2^2)^2} \tag{4.9b}$$

$$b_{n,6} = \frac{2 Z_2}{(1 - Z_2^2)} b_{n,5} + \frac{F_n''(Z_2)}{720(1 - Z_2^2)^2} \tag{4.9c}$$

$$b_{n,7} = \frac{16}{7} \frac{Z_2}{(1 - Z_2^2)} b_{n,6} - \frac{2(n+1)(n+2)(1 - Z_2^2)}{42(1 - Z_2^2)^2} b_{n,5} + \frac{24(1 - 3 Z_2^2)}{42(1 - Z_2^2)^2} b_{n,6} + \frac{F_n'''(Z_2)}{5040(1 - Z_2^2)^2} \quad . \tag{4.9d}$$

Higher order coefficients may be derived in the same way. However, their evaluation becomes increasingly more cumbersome, whereas the accuracy of the analytical solution is impaired if the $Y_n(Z)$ is truncated too early. Thus, in general, numerical integration is recommended.

However, for the particular case when the θ_1 and θ_2 boundaries are symmetrical, as depicted in Figure 2, the analytical solution is considerably simplified. For this case, $Y_1(Z)$ may be obtained in the following simple closed form:

$$Y_1(Z) = \frac{1}{32\, Z_1^6} \{3(2 Z_1^2 - 1)Z + 2(2 - 3Z_1^2)Z^3 - Z^5\} \tag{4.10}$$

Moreover, for $n \geq 2$, the $Y_n(Z)$ Taylor-series expansion, which is given about $Z = 0$ for this case, includes only odd powers of Z, i.e.:

$$Y_n(Z) = \sum_{m=0} b_{n,2m+1} Z^{2m+1} \qquad n \geq 2 \tag{4.11}$$

choosing

$$b_{n,1} = b_{n,3} = 0 \tag{4.12ab}$$

The following values are obtained for subsequent coefficients up to $b_{n,11}$:

$$b_{n,5} = \frac{F_n'(0)}{120} \tag{4.12c}$$

$$b_{n,7} = \frac{120\,((24 - 2(n + 1)(n + 2))b_{n,5} + F_n'''(0)}{5040} \tag{4.12d}$$

$$b_{n,9} = (5040(60 - 2(n + 1)(n + 2))b_{n,7} - 120(n(n + 1)(n + 2)(n + 3) + 360 - 40(n + 1)(n + 2))b_{n,5} + F_n^{V}(0))/362,880 \tag{4.12e}$$

$$b_{n,11} = ((40,642,560 - 725,760(n + 1)(n + 2)b_{n,9} + (423,360(n + 1)(n+2) - 8,467,200 - 5040\, n(n+1)(n+2)(n+3))\, b_{n,7} + F_n^{VII}(0))/39,916,800 \tag{4.12f}$$

Truncation of the $Y_n(Z)$ series after $(b_{n,11}Z^{11})$ is sufficiently accurate, particularly if Z_1 is small.

5. THE VELOCITY AND PRESSURE SERIES.

Substitution for Ψ in Equations (2.12) by its series given in Equation (4.1) yields:

$$V_R(R,Z) \sim -\frac{1}{R^2} \sum_{n=0}^{k} \frac{f_n'(Z)}{R^n} \tag{5.1}$$

$$V_\theta(R,Z) \sim \frac{1}{R^2(1 - Z^2)^{\frac{1}{2}}} \sum_{n=0}^{k} \frac{n f_n(Z)}{R^n} \tag{5.2}$$

Substitution for Ψ in Equation (2.14a) by its series given in Equation (4.1), and integration along a θ = constant line from R = R to R = ∞, yields:

$$P - P_\infty \sim \frac{1}{R^3} \sum_{n=o}^{k} \frac{h_n(Z)}{R^n} \tag{5.3}$$

where $h_n(Z)$ for $o \le n \le k$, are defined by:

$$h_o(Z) = \frac{(1 - Z^2)\, f_o''' - 2Z\, f_o''}{3} \tag{5.4}$$

$$h_{n+1}(Z) = \frac{1}{(n+4)} \{(n+1)(n+2) f'_{n+1} + (1 - Z^2) f'''_{n+1} - 2\, Z\, f''_{n+1} + \sum_{s=o}^{n} [s\, f_s\, f''_{n-s} - (n-s+2) f_s'\, f'_{n-s} - s(n-s) \frac{f_{n-s}\, f_s}{1 - Z^2}]\} \quad \text{for } n \ge 0 \tag{5.5}$$

Since at R = ∞ the flow is certainly creeping, then $\Psi\big|_{R=\infty} = f_o(z)$, and hence Equation (2.14b) gives

$$\frac{\partial P}{\partial Z}\bigg|_{R=\infty} = 0 \tag{5.6}$$

Moreover, from Equation (5.3), it is deduced that:

$$\partial P/\partial R \,\big|_{R=\infty} = 0. \tag{5.7}$$

Hence, P_∞ is a constant for a given flow problem, and Equation (5.3) gives the pressure difference between any two points in the field.

It is remarked that the first term in each of the asymptotic series for V_R, V_θ and P gives the creeping flow solution.

6. DEMONSTRATION CASE.

For demonstration purposes, results are presented for the case where $Z_1 = 0.996$ and $Z_2 = 0.896$ ($\theta_1 = 5°6'$, $\theta_2 = 26°22'$). For both converging and diverging flows, eight terms were retained in the asymptotic expansion (i.e. k = 7).

6.1 Display of Results.

Figure 3 presents the f_o' profile. For creeping flow, this profile gives both the radial-velocity ($V_R = -\frac{f_o'}{R^2}$) and pressure ($P_w - P = \frac{2\, f_o'}{R^3}$)(1) distributions across the cross-section R. [See note]

Note. The creeping flow solution gives: $P - P_\infty = \frac{d}{dZ}[(1 - Z^2) f_o'']/3R^3$. Differentiating the above equation and comparing with Equation (3.1) yields:

$$d\,P\big|_R = -\frac{6\, f_o''.\, dZ}{3\, R^3}$$

Subsequent integration between Z and Z_1 yields:

$$P_w - P = -\frac{2}{R^3}[f_o'(Z_1) - f_o'(Z)] = \frac{2}{R^3} f_o'(Z)$$

where P_w represents the pressure at the wall $Z = Z_1$ which, from the above equation, is also equal to the pressure at the wall $Z = Z_2$.

Figures (4.10) display the remaining f_n' profiles, i.e. for n = 1 - 7.

Figures (11,12) give the corresponding V_R profiles, computed at R = 0.3 and R = 0.5, respectively; at each section R (depicted by $R_N \equiv 1/R$) the velocity profiles for both convergent and divergent flows are displayed, as well as the profile that would be obtained if the inertial terms were neglected (creeping flow solution).

Figure 13 presents the V_θ profile for both converging and diverging flows at R = 0.5 (R_N = 2). The streamline patterns for converging and diverging flows are revealed in Figures 14 and 15, respectively.

Figures (16-19) show the h_n profiles for n = 1,3,5, and 7. The corresponding cross-stream pressure-distribution at R = 0.5, is given, for both converging and diverging flows, in Figure 20; whereas, the diverging-flow streamwise pressure-distribution along the inner wall, is displayed in Figure 21. A critical dimensionless radius R_c is indicated which marks the value of R beyond which $\partial P/\partial R$ changes sign.

6.2 *Discussion of Results.*

The radial velocity profile:

(i) Creeping flow: The creeping flow profile, which is expressed by $-\frac{f_o'}{R^2}$, is the same for converging and diverging flows. The profile is skew, since the skin-friction area at the inner wall is smaller than the area at the outer wall.

(ii) Flow with inertia: Although the functions f_n' are identical for converging and diverging flows, the velocity profiles are different for $k \geq 1$. This is a consequence of the q sign convention, which is positive for diverging flows and negative for converging flows. Thus, the terms exhibiting odd powers of R will yield contributions of opposite signs in converging and diverging flows.

Inspection of the f_n' profiles for $o \leq n \leq k$ indicates the direction in which the profiles develop as R changes; of course, as R decreases, the higher order terms become more influential. For diverging flow, where R^n is always positive, comparison of the f_n' profiles for $n \geq o$ shows that as R decreases, the velocity profiles become more peaked, and that for sufficiently small values of R, a recirculation zone would exist near the outer wall. For converging flow, where R^n is negative for odd values of n, the development of the V_R profile with decreasing R is not deduced as easily as for

diverging flow. However, if one focuses attention on the first two terms only, then it is immediately apparent that the effect of the inertia terms would be to flatten the creeping flow profile, and that the lower the value of R, the flatter the profile, until eventually a boundary-layer type profile is obtained.

Inspection of the converging and diverging flow V_R profiles calculated at $R_N = 2$ and $R_N = 3.3$ shows that they confirm to the previous observations. Comparison of the converging and diverging flow profiles at a given R, against the creeping flow one reveals that the diverging flow profiles deviate considerably more from the creeping flow profiles than the corresponding converging flow ones. Moreover, comparison of the diverging flow profile at $R_N = 3.3$ against the one at $R_N = 2$ shows marked differences. Extrapolation beyond $R_N = 3.3$ indicates that recirculation near the outer wall should be expected at slightly larger values of R_N. It must be mentioned however, that $R = 0.3$ ($R_N = 3.3$) is roughly the smallest value of R for which the asymptotic series will converge for the full eight terms.

The Ψ pattern and V_θ profiles:

At large values of R, the streamlines for both converging and diverging flows are radial straight lines. However, as R decreases the deviation from radiality becomes more pronounced, particularly for diverging flow. Thus at large values of R, V_θ is negligible; whereas, at small values of R, V_θ is not negligible. Since for a given R, the radial inclination of the streamlines is larger for diverging than for converging flows, the magnitude of V_θ is also larger for diverging flows.

The pressure profiles:

(i) Cross-stream distribution: For $n \geq 1$ the $h_n(Z)$ profiles change monotonically with n; thus they imply a monotonic change of the diverging flow profile with R. In particular, it is noticed that whereas for creeping flow the pressure at both walls is equal, for diverging flow the pressure at the outer wall is larger that at the inner one, the difference increasing with decreasing R.

Comparison of the converging and diverging flow profiles at the same R shows that the latter is much more peaked, the same as with the V_R profile.

(ii) Streamwise distribution: Differentiation of Equation (5.7) with respect to R yields:

$$\frac{\partial P}{\partial R} \sim -\frac{3h_o}{R^4} - \frac{4h_1}{R^5} \ldots - (n+3)\frac{h_n}{R^{n+4}} \ldots - \frac{10\,h_7}{R^{11}} \qquad (6.1)$$

Since $h_o(Z)$ is positive and $h_n(Z)$ is negative for $n \geq 1$, thence it is seen that for diverging flow, the first term in the series (creeping flow solution) tends to give a pressure-drop which is required to overcome the viscous forces; whereas, the remaining terms (inertia terms contributions) tend to raise the pressure due to the diffuser effect of the passage. Thus $\frac{\partial P}{\partial R}$ will be positive for small values of R, and negative for large values of R. The value of R at which $\frac{\partial P}{\partial R} = 0$ is designated R_c and indicated in Figure 21.

For converging flow, the first two terms will give a pressure drop, whereas the remaining ones will alternate in sign. Thus it should be expected that $\partial P/\partial R$ will be negative, obviously due to the combined effects of viscous-friction and conversion of pressure-energy into kinetic-energy.

7. CONCLUSION.

In this paper an asymptotic series solution is obtained for low Reynolds-number flow between two co-axial cones with a common vertex. The first term in the asymptotic series gives the creeping flow solution, which, to the best of the authors knowledge, is presented here in closed form for the first time. Except for a special case where another term was also obtained in closed form, subsequent terms of the asymptotic series contain functions which are presented in infinite series forms. Theoretically, the evaluation of these functions may be performed manually; however, in general, it is recommended to resort to computer aid in order to solve directly the ordinary differential equations derived for these functions. It must be emphasized, though, that the computational effort involved therein is much less than what would be required for the numerical solution of the non-linear Navier-Stokes equations. Moreover, since the functions to be evaluated numerically are universal for a given set of cone angles, the computations need only be performed once for a given geometry.

The geometrical configuration considered here is encountered in fluid ducts of many applications. Whenever the Reynolds-number of the flow is small, the mathematical model presented here should yield useful predictions of the velocity and pressure distributions.

Appendix A: Solution of the $f_o(Z)$ equation.

Integrating Equation (3.1) twice w.r.t.Z. yields:

$$(1 - Z^2)\, f_o'' + 6\, f_o = A_o\, Z + B_o \qquad (A.1)$$

where A_o and B_o are constants.

The corresponding homogeneous equation

$$(1 - Z^2)\ \bar{f}_o'' + 6\ \bar{f}_o = 0 \tag{A.2}$$

represents a special case of the more general differential Equation (B.1). Hence, the complementary function is given by

$$f_o(Z) = \frac{(Z^2 - 1)}{6}\ [C_o\ P_2'(Z) + D_o\ Q_2'(Z)] \tag{A.3}$$

where C_o and D_o are constants.

A particular solution of Equation (A.1) is

$$f_o(Z) = \frac{A_o Z + B_o}{6} \tag{A.4}$$

Hence, according to the general theory of linear differential equations, the general solution of Equation (A.1) is expressed by

$$f_o(Z) = \frac{1}{6}\ (Z^2 - 1)[C_o\ P'_2(Z) + D_o\ Q_2'(Z)] + A_o\ Z + B_o \quad . \tag{A.5}$$

With the help of Equation (B.3), it may also be obtained that

$$f_o'(Z) = \frac{A_o}{6} + C_o\ P_2(Z) + D_o\ Q_2(Z) \quad . \tag{A.6}$$

Appendix B: Solution of D.E. for the Integral of Legendre-Function.

The solution of the differential-equation

$$(1 - Z^2)\ G_n''(Z) + n(n + 1)\ G_n(Z) = 0 \tag{B.1}$$

where $G_n(Z)$ is a function of Z, was derived by the authors as follows:

differentiating Equation (B.1) w.r.t.z. yields

$$(1 - Z^2)\ G_n'''(Z) - 2\ Z\ G_n''(Z) + n(n + 1)\ G_n'(Z) = 0 \tag{B.2}$$

which is the Legendre differential-equation for the function $G_n'(Z)$. Hence, $G_n'(Z)$ is given by

$$G_n'(Z) = A_n\ P_n(Z) + B_n\ Q_n(Z) \tag{B.3}$$

where A_n and B_n are constants.

In passing, it is mentioned that, because the integration of the Legendre functions on the right-hand side of Equation (B.3) yields the solution of the differential-equation (B.1), the authors refer to the latter equation as the differential-equation for the integral of Legendre-functions. However, since differentiation is always more feasible than integration, the function $G_n(Z)$ is derived by first differentiating Equation (B.3) w.r.t.z. to yield

$$G_n''(Z) = A_n\ P_n'(Z) + B_n\ Q_n'(Z) \tag{B.4}$$

then substitution of the right-hand side of Equation (B.4) for $G_n''(Z)$ in Equation (B.1)

produce

$$G_n(Z) = -\frac{(1 - Z^2)}{n(n+1)} \left[A_n P_n'(Z) + B_n Q_n'(Z) \right] . \qquad (B.5)$$

Appendix C: Solution of the Homogeneous Differential Equation for $f_n(Z)$

The homogeneous differential equation for $f_n(Z)$ is expressed by

$$(1-Z^2)^2 \bar{f}_n^{IV} - 4Z(1-Z^2)\bar{f}_n''' + 2(n+1)(n+2)(1-Z^2)\bar{f}_n'' + n(n+1)(n+2)(n+3).\bar{f}_n = 0 . \qquad (C.1)$$

Equation (C.1) may be rearranged in the form:

$$(1-Z^2) \frac{d^2}{dZ^2} [(1-Z^2) \bar{f}_n'' + n(n+1) \bar{f}_n] + (n+2)(n+3) [(1-Z^2) \bar{f}_n'' + n(n+1)\bar{f}_n] = 0 \qquad (C.2)$$

Thus a solution of the differential-equation

$$(1 - Z^2) \bar{f}_n'' + n(n+1) \bar{f}_n = 0 \qquad (C.3)$$

is also a solution of (C.2). From Appendix B, the solution of this equation is

$$\bar{f}_n = -\frac{(1 - Z^2)}{n(n+1)} \{A_n P_n' + B_n Q_n'\} \qquad (C.4)$$

where A_n and B_n are arbitrary constants.

Equation (C.1) can also be rewritten in the form

$$(1-Z^2) \frac{d^2}{dZ^2} [(1-Z^2) \bar{f}_n'' + (n+2)(n+3) \bar{f}_n] + n(n+1)[(1-Z^2) \bar{f}_n'' + (n+2)(n+3) \bar{f}_n] = 0 . \qquad (C.5)$$

Thus a solution of the differential-equation

$$(1 - Z^2) \bar{f}_n'' + (n+2)(n+3) \bar{f}_n = 0 \qquad (C.6)$$

is also a solution of (C.1). From Appendix B, this solution is given by

$$\bar{f}_n = \frac{-(1 - Z^2)}{(n+2)(n+3)} \{C_n P_{n+2}'(Z) + D_n Q_{n+2}'(Z)\} \qquad (C.7)$$

where C_n and D_n are arbitrary constants.

Since the functions $P_n(Z)$, $Q_n(Z)$, $P_{n+2}(Z)$ and $Q_{n+2}(Z)$ are independent, and thus offer four independent solutions to the fourth-order linear differential-equation (C.1), then the general solution of this equation is

$$\bar{f}_n(Z) = -(1 - Z^2) \left\{ \frac{A_n P_n'(Z) + B_n Q_n'(Z)}{n(n+1)} + \frac{C_n P_{n+2}'(Z) + D_n Q_{n+2}'(Z)}{(n+2)(n+3)} \right\} . \qquad (C.8)$$

Moreover, considerations of Equation (B.3) yield

$$\bar{f}_n'(Z) = A_n P_n(Z) + B_n Q_n(Z) + C_n P_{n+2}(Z) + D_n Q_{n+2}(Z) . \qquad (C.9)$$

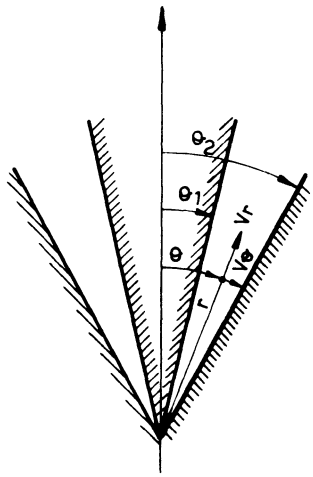

Fig. 1 geometry of Problem Investigated

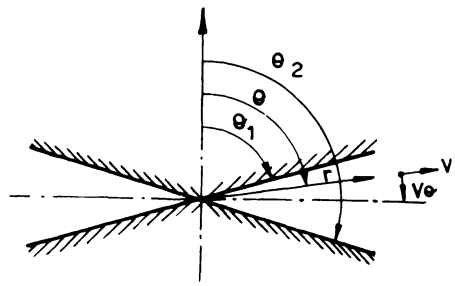

Fig. 2 The Symmetrical Case

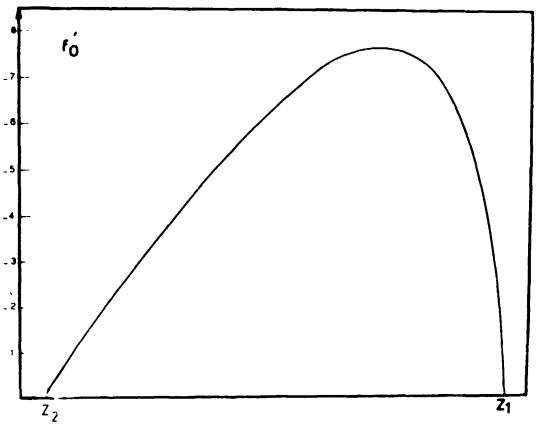

Fig. 3 f_o' profile

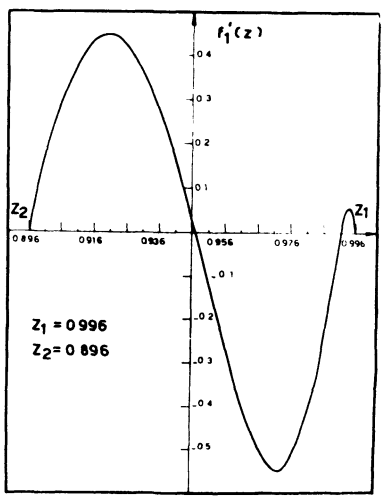

Fig. 4 f_1' profile

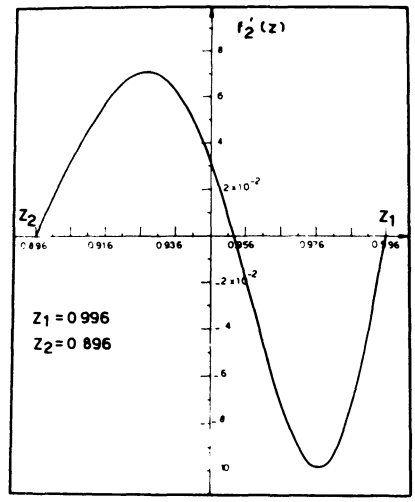

Fig. 5 f_2' profile

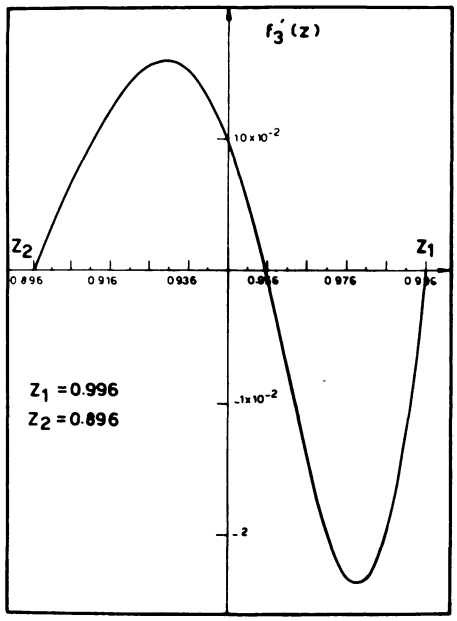

Fig. 6 f_3' profile

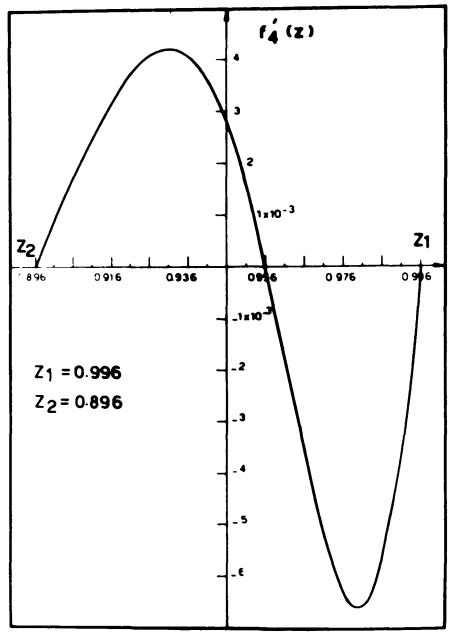

Fig. 7 f_4' profile

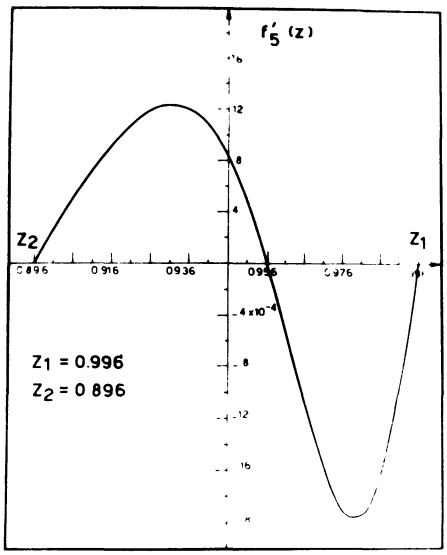

Fig. 8 f_5' profile

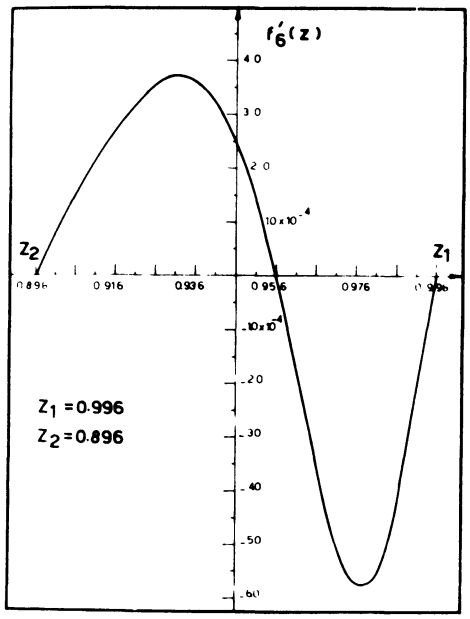

Fig. 9 f_6' profile

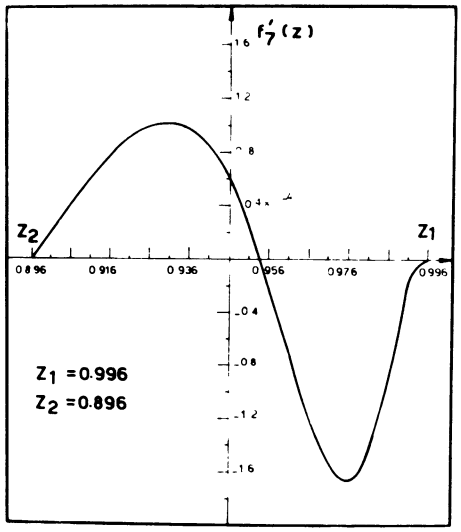

Fig.10 f_7' profile

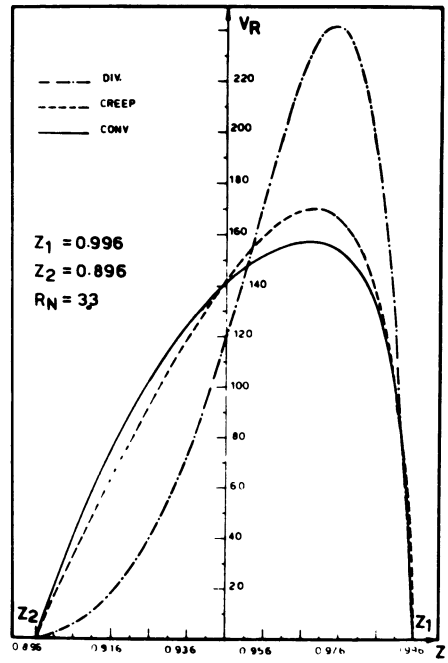

Fig.11 V_R profile at R = 0.3

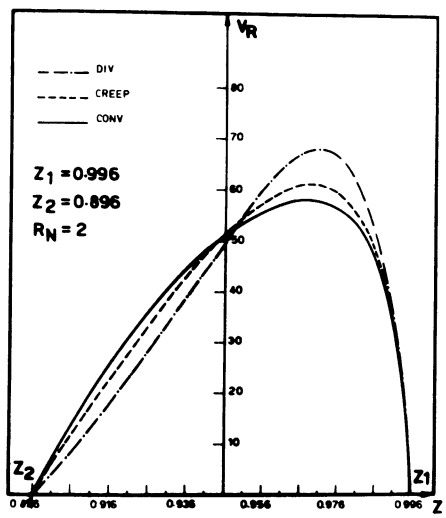

Fig.12 V_R profile at R = 0.5

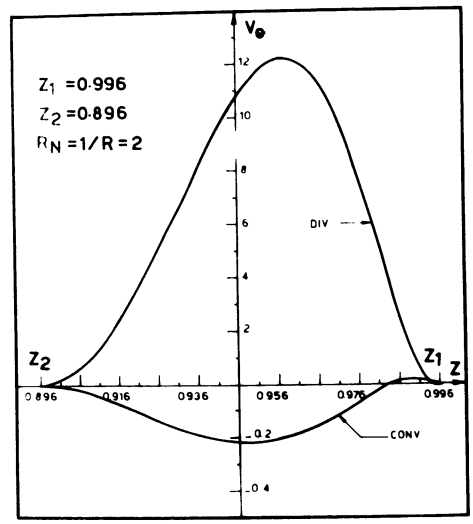

Fig.13 V_θ profile at R = 0.5

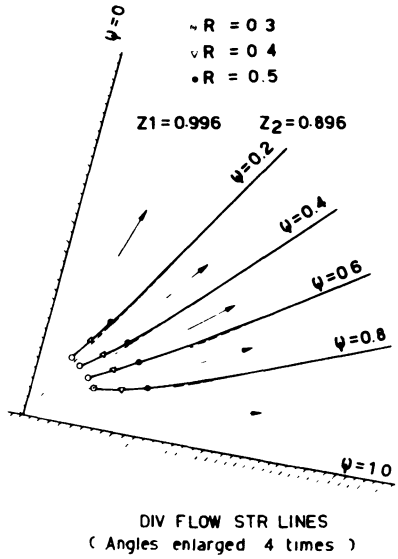

Fig.14 div. flow streamlines

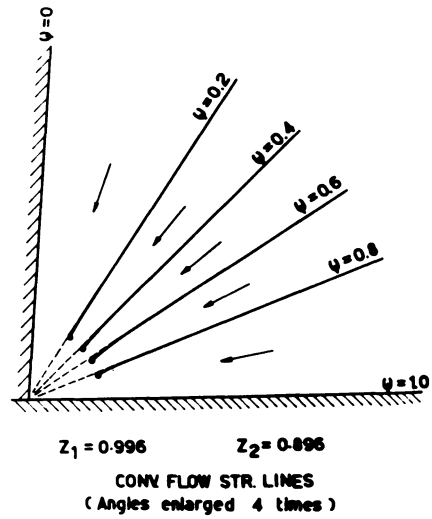

Fig.15 conv. flow streamlines

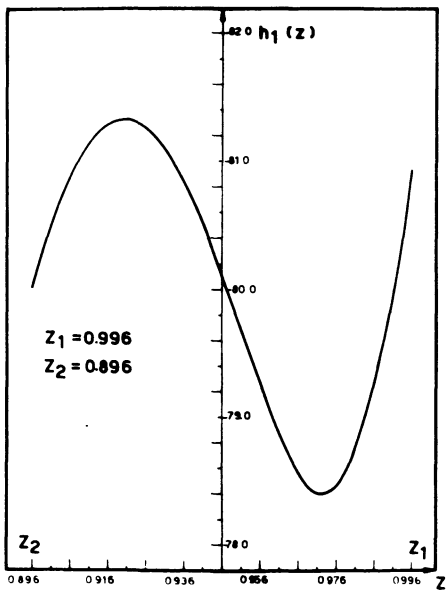

Fig.16 h_1 profile

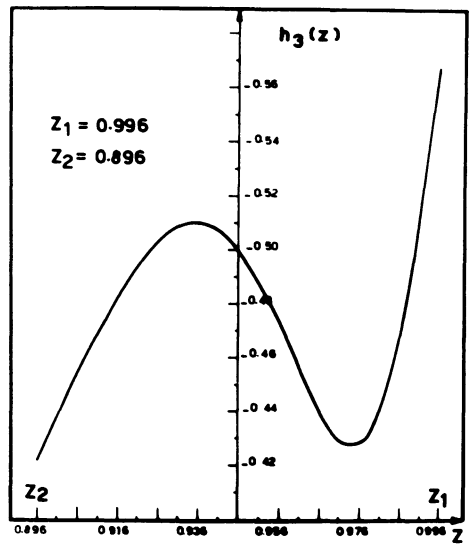

Fig.17 h_3 profile

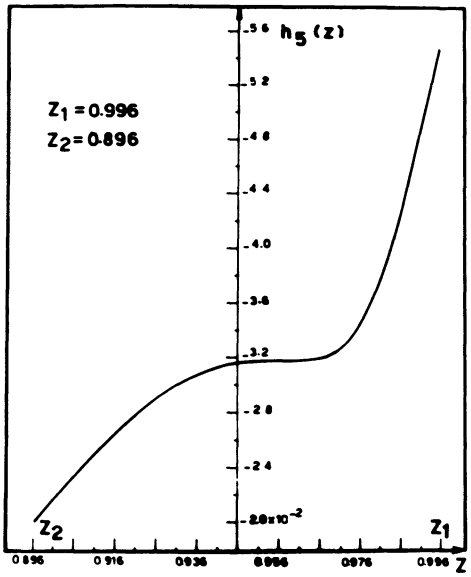

Fig.18 h_5 profile

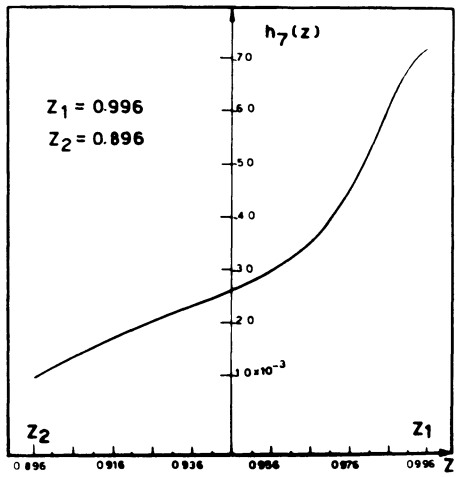

Fig.19 h_7 profile

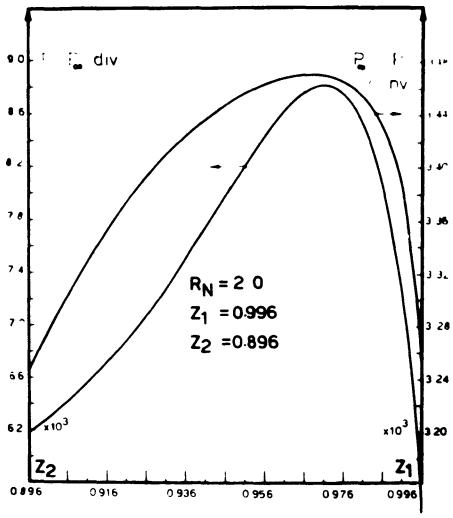

Fig.20 Cross-stream P profile

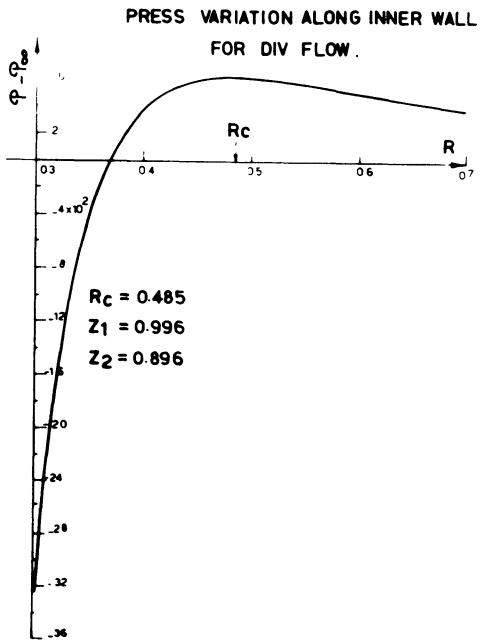

Fig.21 Streamwise P variation

REFERENCES

1. MORSE, P.M. and FESHBACH, H. Methods of Theoretical Physics, Part I, McGraw-Hill, (1953), p. 434-437.

2. PEUBE, J.L. "Sur L'ecoulement radial permanent d'un fluide visqueux incompressible entre deux plans paralleles fixes", J. de Mechanique, vol. II, No. 4 (1963), p. 377-394.

3. ACKERBERG, R.C. The Viscous Incompressible Flow Inside a Cone, J. Fluid Mech. vol. 21, Part I (1965), p. 47-81.

4. RICE, W. and McALISTER, K.W. Laminar Throughflow of a Newtonian Fluid between Coaxial Rotating Cones, Trans. of the ASME 210/March (1970).

5. ABRAMOWITZ, M. and STEGUN, I.A. Handbook of Mathematical Functions, Dover Publications (1965), p. 331-335.